UNITED NATIONS UNIVERSITY
UNU-GTP
Geothermal Training Programme

Orkustofnun, Grensasvegur 9,
IS-108 Reykjavik, Iceland

Reports 2016
Number 13

ANALYSIS OF WELL TESTING, TEMPERATURE AND PRESSURE IN HIGH-TEMPERATURE WELLS OF ALUTO-LANGANO, ETHIOPIA

Mesay Fekadu Biru
Ethiopian Electric Power – EEP
Kirkos Kifle Ketema, Wereda 07, House No. 944/05
Meba Building, P.O. Box 15881
Addis Ababa
EHIOPIA
abushmech@gmail.com

ABSTRACT

Drilling in Aluto-Langano geothermal field started in 1981 with the aim of harnessing steam for electricity power production. Eight wells were drilled between 1981 and 1986, thereof four productive, one reinjection and three non-productive wells. Recently, between 2013 and 2015, two directional wells were drilled and they are still undergoinging different measurements and tests. Measurements from the wells, LA-9D and LA-10D, as well as from an older one, LA-3, were analysed and are presented in this report. Results from analyses of injection tests for wells LA-3 and LA-10D are characterized by having fairly good transmissivity and storativity values and the injectivity indices are rather low. The evaluated fluid enthalpy for wells LA-9D and LA-10D is in the range of 1600-2200 kJ/kg, with steam flow ranging from 5 to 9 kg/s with separation pressure of 1 bar-a as well as with separation pressure of 5 bar-a of Aluto-Langano pilot power plant.

Formation temperatures of wells LA-9D and LA-10D were estimated by extrapolation of temperature logs from their warm up periods. The results suggest that the reservoir temperature is in the range of 300-315°C and reservoir pressure in the range of 85-100 bar for both wells.

1. INTRODUCTION

Ethiopia is one of the East African countries with the most significant geothermal resources. Exploration of the resources started in 1969 and they have been investigated gradually. A total of 10 wells have already been drilled in one of the most promising fields, the Aluto-Langano geothermal field, but the field has only been utilized to a small extent.

In this report the results of analyses conducted on measurements from the Aluto-Langano geothermal field are introduced. From this area, wells LA-3, LA-9D and LA-10D were selected for studying. Different types of analyses were performed including simulations of injection tests from the end of drilling of LA-3 and LA-10D, as well as estimation of formation temperature, initial pressure and analysis of discharge testing from directionally drilled wells LA-9D and LA-10D.

The injection test simulation was made by using Welltester software, based on non-linear regression

(Júlíusson et al., 2008; Marteinsson, 2016). The injectivity index is the first parameter analysed and is a simple relationship between change in flow and change in pressure, reflecting the capacity of a well or how open it is to the surroundings, which is useful for determining whether a well is sufficiently open to be a successful producer, if it should be stimulated or if drilling should possibly be continued to look for better feed zones at deeper levels.

Formation temperature estimations were obtained by using the Berghiti software developed at ISOR – Iceland GeoSurvey (Helgason, 1993; Marteinsson, personal communication). Formation temperature estimation is important to increase the knowledge about a geothermal system for decision making when selecting new sites and for developing conceptual models. The initial pressure is also obtained by using Predyp from ICEBOX software (Arason et al., 2004). Discharge test analysis is obtained by using Lip from ICEBOX software.

Discharge data from LA-9D and LA-10D were analysed at different wellhead pressures.

A short description of Aluto-Langano geothermal system is given in Section 2. Injection tests from two wells were analysed and discussed in Section 3. Temperature and pressure profiles during warm up period were analysed to determine the formation temperature and initial pressure and the process and results are introduced in Section 4 and, finally, the result of discharge testing is analysed followed by discussion and conclusion in Sections 5 and 6.

1.1 Geothermal system

Geothermal resources are distributed throughout the planet. Even though most geothermal systems and the greatest concentration of geothermal energy are associated with the Earth‘s plate boundaries, geothermal energy can be found in most countries. It is highly concentrated in volcanic regions, but can also be found as warm groundwater in sedimentary formations worldwide as low-temperature systems (Axelsson, 2012). Geothermal systems are governed by the surface and subsurface hydrological pattern, heat source and surface activity associated with the geothermal resource. While the term geothermal field is considered to refer to the area of geothermal activity on surface, intended as a geographic description, it is regarded as a component of the geothermal system. The geothermal reservoir is the section in the geothermal system that can be economically exploited for energy utilization.

Geothermal systems exist in different forms and are classified on the basis of reservoir temperature, enthalpy, physical state, geological settings and nature (Axelsson, 2012). Low-temperature systems (<150°C), are referred to as low-enthalpy systems (<800 kJ/kg). This type of geothermal systems exists e.g. in sedimentary basins with permeability at great depth and is classified as liquid-dominated geothermal systems. High-temperature systems (>200°C) may also be described as high-enthalpy systems (>800 kJ/kg). They are mostly characterised by active volcanism, the heat source being shallow magma, intrusions or dykes.

1.2 Geothermal wells

Geothermal wells play a key role in research and development of geothermal systems. Geothermal wells provide access for direct testing and measurements of the systems. They are vital components in both geothermal research and utilization, since they provide essential access for both energy extraction and information collection (Axelsson, 2013). Geothermal wells can be classified as low-temperature or high-temperature wells. A low-temperature (liquid-dominated) well produces liquid water at wellhead while a high-temperature well in which the flow from feed zone(s) is liquid or two-phase produces either a two-phase or dry steam at wellhead (Grant and Bixely, 2011).

There are many types of geothermal wells, some of them are described in the following. Temperature gradient wells are designed as slim and shallow, typically less than 100 m in depth, drilled in the early stage of geothermal research. Their main purpose is to determine the temperature gradient near surface at shallow depth. Another type are the exploration wells which are drilled during the exploration phase, usually deeper than gradient wells to hit the geothermal reservoir with the purpose of exploring its conditions. The production wells have the main purpose of facilitating the geothermal energy extraction from the reservoir but are also used for gaining further information about the reservoir. The step-up wells are drilled to extend the confirmation of a particular geothermal reservoir while the make-up wells are used to make up for either damaged production wells due to scaling or collapse or regular declining output of production wells with time. The injection wells are used for injecting water back into the geothermal system which helps maintaining production capacity, for environmental management and decreasing pressure drops. The monitoring wells are used for management purposes, i.e. for monitoring how the geothermal system reacts to the production (Axelsson, 2013).

2. ALUTO-LANGANO GEOTHERMAL SYSTEM

2.1 Location and geological setting of Aluto-Langano

Ethiopia is one of the East African countries with the most significant geothermal resources, and launched a long-term geothermal exploration in 1969. Over the years a good inventory of the potential target areas has been built up and more than 23 prospects are judged as having potential for electricity production (Teklemariam, 1996; Teklemariam et al., 1996).

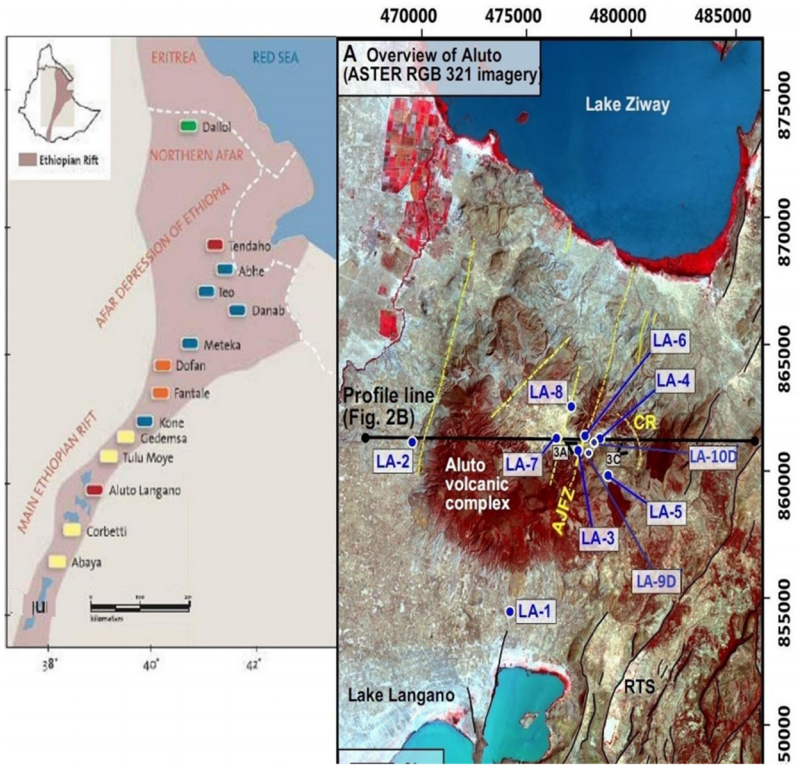

FIGURE 1: Main Ethiopian rift valley to the left and Aluto volcanic complex to the right (Hutchison et al., 2015)

The geothermal resources are present in the main Ethiopian Rift System and in the Afar depression, which are parts of the Great East Africa Rift System. More than sixteen geothermal prospects are located along this rift that are believed to have the potential for electricity production. Aluto-Langano, Tendaho, Corbetti, Abaya, Tulumoye-Gedemsa, Dofan and Fantale (Figure 1) are few of the prospect areas in which detailed exploration study and drilling have started due to their expected potential and their strategic location relative to the national electric grid (Worku Sisay, 2016).

2.2 Surface geology of Aluto-Langano

Aluto volcanic complex covers an area of about 100 km^2 between lakes Langano and Ziway (Figures 1 and 2) and rises to elevation of 690 m above the surrounding Adami-Tullu plain which has an elevation

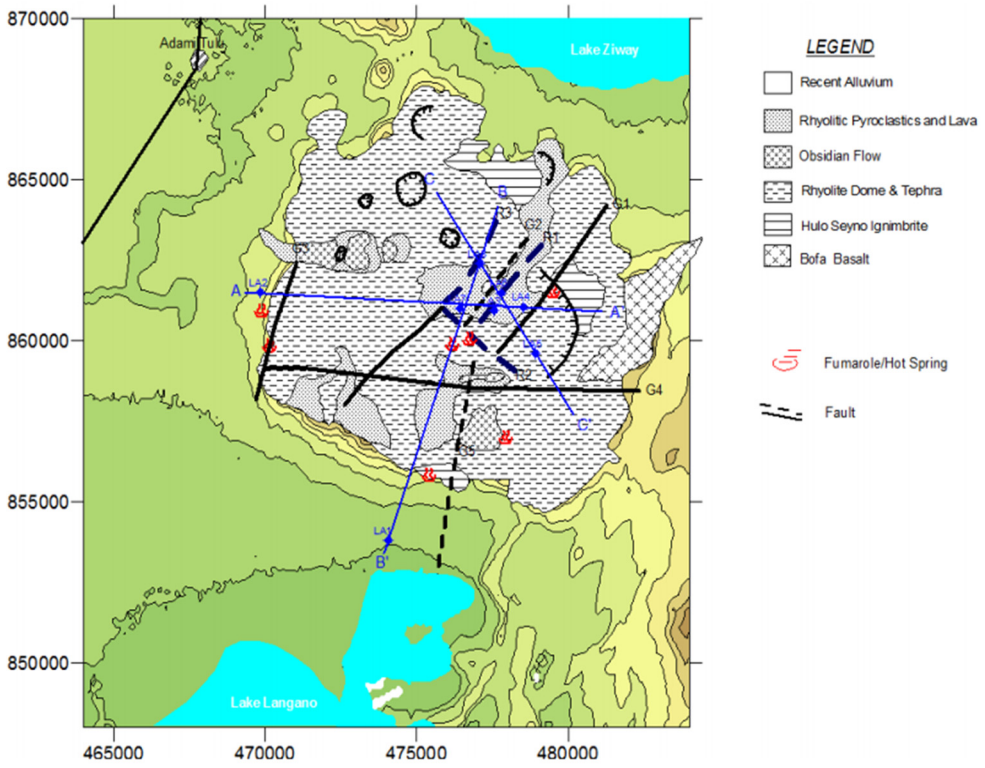

FIGURE 2: Geological map of Aluto-Langano geothermal field and the Wonji Fault Belt (Hutchison et al., 2015)

of about 1600 m a.s.l. The broad truncated base and a summit caldera are 6 km by 9 km (with an area of 37 km^2) elongated in a WNW direction have formed a basin of internal drainage (Worku Sisay, 2016). Volcanic activity at the Aluto volcanic centre mostly occurred in the Quaternary with earlier sub-lacustrine eruptions. The activity is initiated with a rhyolite dome building phase intervened by explosive pyroclastic pumice eruptions and a major caldera forming pyroclastic eruption. The ignimbrite is now exposed on the flanks of the Aluto volcanic massif as pumices ignimbrites and sub-aqueous pumices tuff with minor intercalations of lacustrine sediments. Post-caldera collapse rhyolite flows, domes with minor pyroclastic products formed along the NE-SE segment of the Aluto Caldera rim on a basement of pumices ignimbrites and older rhyolite. Predominantly rhyolite post-caldera lava and pyroclastic have erupted from numerous craters with all vents showing a clear control by either the caldera ring fracture or the NNE trending faults of the Wonji Fault Belt (WFB). The northern segment of the centre is characterised by large rhyolite domes and flows, which do not show a marked structural control. Minor basaltic lavas have erupted from the north-northeast trending faults east of Aluto massif. The Aluto caldera is covered by alluvial sediments (Teklemariam and Beyene, 2000).

2.3 Exploration drilling

Aluto-Langano is the first geothermal field in Ethiopia to be exploited. In this area, eight deep exploration wells (LA-1 to LA-8) (Figure 3) were drilled from 1981 to 1986 with a maximum depth of 2500 m, reaching temperatures of up to 335°C (Teklemariam and Beyene, 2000). Wells LA-1 and LA-2 were drilled at the southern and western flanks of Aluto Volcanic Complex (AVC), respectively (Figure 3), and are characterized by low temperature and permeability. Wells LA-3 to LA-8 were sited on top of Aluto-Langano in the south-eastern part of the area. LA-3 and LA-6 were drilled in the most active fault system, Wonji Fault Belt (WFB) (Figure 2), trending in north-northeast direction, and where maximum temperature recorded were 315 and 335°C, respectively (UNDP, 1986). LA-4 and LA-5 were drilled in the eastern part of Wonji Fault Belt and LA-7 and LA-8 in the western part (Figure 3).

The first 7.2 MWe pilot power plant was installed in the Aluto-Langano field by the Ethiopian Electric Power Corporation and connected to the national power grid in May 1998. It was started by connecting four production wells, LA-3, LA-4, LA-6 and LA-8, and one reinjection well, LA-7 (Teklemariam and Beyene, 2000). The expected capacity of this geothermal field was 30 MW_e for 30 years. The pilot power plant has not been in full operation due to problems related to the production wells (e.g. decline of well pressures, scaling and wellhead valve problems) and problems related to the power plant involving cooling tower fan breakdowns, pentane leakage from the heat exchangers and so on. According to Kebede (2012), the plant has been partially renewed and started to produce 4 MW_e in 2007. Recently, two exploration wells have been drilled, LA-9D and LA-10D, using a rig owned by the Geological Survey of Ethiopia. LA-9D and LA-10D are the first directional wells in Ethiopia and both wells are in testing phase.

Information about wells LA-3 to LA-10D is given in Table 1.

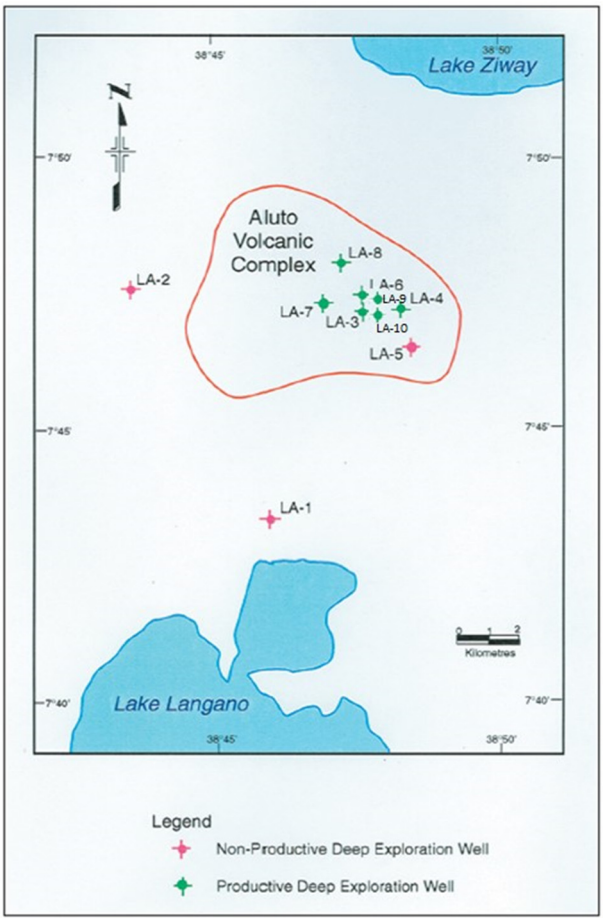

FIGURE 3: Wells LA-1 to LA-10D located in Aluto-Langano geothermal field

TABLE 1: Information about exploration wells in Aluto-Langano geothermal field (P: Productive; NP: Non productive; RW: Reinjection well)

Well	LA-3	LA-4	LA-5	LA-6	LA-7	LA-8	LA-9D	LA-10D
Drilled depth (m)	2114	2062	1867	2203	2448	2500	1921	1950
Elevation (m a.s.l.)	1921	1956	2037	1962	1891	1895	1963	1960
Permeable zones (m)	2000-2121	1445-1800	-	2000-2200	2100-2300	2300-2500	760-1350	920-1760
Maximum T (°C)	322	240	210	335	228	284	308	310
Status of the well	P	P	NP	P	RW	P	P	P
Time of drilling	21/1/83-13/6/83	6/7/83-23/10/83	15/11/83-11/3/84	24/3/84-2/7/84	12/7/84-21/10/84	26/10/84-13/5/84	12/11/13-01/02/15	25/06/15-02/10/15

3. INJECTION WELL TESTING

3.1 Introduction of pressure transient analysis

Immediately after completion of geothermal well drilling, well testing is conducted in order to assess the conditions of a well and the properties of the reservoir intersected by the well, by subjecting it to injection or production. During an injection test, the response of a reservoir to changing injection rate is monitored. A change in flow rate usually results in changes in pressure which can be measured. Examples of parameters that control the reservoir response are storativity, transmissivity (permeability),

wellbore storage, wellbore skin, fracture properties and reservoir boundaries. A mathematical model is commonly set up to simulate the pressure transient response in the well and the reservoir caused by an instantaneous step change in injection or production. The mathematical model depends on values selected for properties characterising the reservoir and by iterating these values such that the modeled response fits the observed data though one can infer the characteristic properties of the reservoir (Horne, 1995). Pressure diffusion equation is the basis of all models in well testing theory or pressure transient analysis.

The pressure diffusion equation is used to calculate the pressure (p) in the reservoir at a certain distance (r) after a given time (t) of an injection (or production) well receiving or producing fluid at specific rate (Q), starting at time $t = 0$. The pressure diffusion equation is derived by combining the conservation of mass law, Darcy's law and the equation of state of the fluid.

The following assumptions are made before the equation is derived (Horne, 1995; Haraldsdóttir, 2016):

- Horizontal radial flow;
- Darcy's law applies;
- Homogeneous and isotropic reservoir;
- Isothermal conditions;
- Uniform thickness of reservoir, h;
- Single-phase flow;
- Small pressure gradients;
- Small and constant compressibility, c_t;
- Constant porosity, φ;
- Constant fluid viscosity, μ;
- Constant permeability, k.

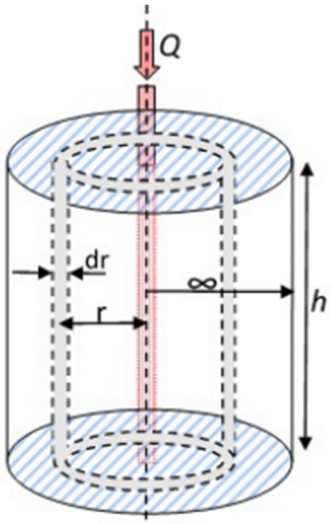

FIGURE 4: Radial flow through a cylindrical shell around a well (Haraldsdóttir, 2016)

The law of conservation of mass says that mass flow in minus mass flow out equals mass rate of change within the control volume. Consider the flow through a cylindrical shell of thickness *dr* situated at a distance r from the centre of the cylinder in Figure 4.

Then applying the law of conservation of mass leads to:

$$\left(\rho Q + \frac{\delta(\rho Q)}{\delta r}dr\right) - \rho Q = 2\pi r \frac{\delta(\varphi \rho h)}{\delta t}dr \quad \text{or}$$

$$\frac{\delta(\rho Q)}{\delta r} = 2\pi r \frac{\delta(\varphi \rho h)}{\delta t} \tag{1}$$

where ρ = Density (kg/m^3);
φ = Porosity (ratio $0<\varphi<1$);
Q = Volumetric flow rate (m^3/s);
r = Radial distance (m) from the well;
t = Time (s);
h = Reservoir thickness (m).

Darcy's law or law of conservation of momentumin radial form is:

$$\left(Q = \frac{2\pi r h k}{\mu}\frac{\delta p}{\delta r}\right) \tag{2}$$

where p = Pressure (Pa);
μ = Dynamic viscosity (Pa. s);
k = Formation permeability (m^2).

The equation of state (compressibility at constant temperature) can be expressed as:

$$c_t = c_w \emptyset + (1-\emptyset)c_r \quad \text{where } c_w = \frac{1}{\rho}\frac{\delta\rho}{\delta p} \quad and\ c_r = \frac{1}{1-\emptyset}\frac{\delta\emptyset}{\delta p} \tag{3}$$

where c_w = Fluid compressibility (Pa^{-1})
c_r = Rock or formation compressibility (Pa^{-1})
c_t = Total compressibility (Pa^{-1})

By combining Equations 1, 2, and 3, we obtain the pressure diffusion equation:

$$\frac{1}{r}\frac{\partial}{\partial r}\left(\frac{r\,\partial p(r,t)}{\partial r}\right) = \frac{\mu c_t}{k}\frac{\partial p(r,t)}{\partial t} = \frac{S}{T}\frac{\partial p(r,t)}{\partial t} \tag{4}$$

$$\frac{\partial^2 p}{\partial r^2} + \frac{1}{r}\left(\frac{\partial p(r,t)}{\partial r}\right) = \frac{\mu c_t}{k}\frac{\partial p(r,t)}{\partial t} = \frac{S}{T}\frac{\partial p(r,t)}{\partial t}$$

Equation 4 is the basic equation for well testing. Solutions for this equation can be obtained for different regimes depending on the initial and boundary conditions but that is beyond the scope of this project.

3.2 Injection well test process and analysis

An injection test is done by lowering a pressure tool to a selected depth near to a major permeable zone in the well. Water is pumped into the well at different pumping rates. In some cases constant injection rate is applied for a while before starting the test, allowing the pressure to stabilize, but in other cases there is no injection until the step test starts, e.g. in the injection tests from Aluto-Langano. The first pumping rate in the test is held constant to allow the pressure to stabilize. The pumping rate is then changed stepwise with the duration of each step long enough to allow the pressure in the well to stabilize again. This process is repeated for several pumping rates. In some countries the pump is turned off at the end of the well test and the well is monitored and allowed to return to its natural pressure, which is the so called fall-off test. During all this process, the well pressure is recorded as a function of time.

The analysis of the injection test is done using the software Welltester vers. 2 (WT) (Marteinsson, 2016) to handle data manipulation, to analyse well tests (mainly multi-step injection tests) and to present the results both graphically and in tables. The software works like this: (Haraldsdóttir, 2016; Marteinsson, 2016).

- Initial parameters: The reservoir temperature, rock type and porosity are fed into the program and the initial pressure is deduced by WT. These values are used to calculate approximate values of the dynamic viscosity of the reservoir fluid and the total compressibility of the rock matrix and the fluid. The wellbore radius which is the average radius of the well below the production casing to reservoir depth is also fed into the program.
- Set steps: The initiation time of injection steps is selected on the graph.
- Modify: This step is designed to clean, correct and resample the data.
- Model: In this step, the most appropriate model for the reservoir being investigated is selected. To achieve this, the derivative plot is used along with the pressure data as a function of time on graphs with log-log scale as well as linear and log-linear scale.

The main parameters deduced from the Welltester simulation are explained in the manuals of WellTester and Welltester V2 (Júlíusson et al., 2008; Marteinsson, 2016) as follows:

Transmissivity, T, describes the ability of the reservoir to transmit fluid, hence largely affecting the pressure gradient between the well and the reservoir. Its physical formulation is kh/μ, where k is the effective permeability of the reservoir, h is the reservoir thickness and μ is the dynamic viscosity of the active reservoir fluid.

Storativity, S, defines the volume of fluid stored in the reservoir per unit area per unit increase in pressure [m^3/(Pa m^2) or m/Pa]. How fast the pressure can travel within the reservoir depends on the storativity of the reservoir. Storativity depends on fluid compressibility, or $S = c_t h$. It varies greatly between reservoir types, i.e. liquid dominated vs. two phase or dry steam. Common values for liquid-dominated geothermal reservoirs are around 10^{-8} m^3/(Pa m^2) and 10^{-5} m^3/(pa m^2) for two-phase reservoirs.

The skin factor, s, is a variable used to quantify the permeability of the volume immediately surrounding the well. This volume is often affected by drilling operations, being either damaged (e.g. because of drill cuttings clogging the fractures) or stimulated (e.g. due to erosion or extensive fracturing around the well). For damaged wells the skin factor is positive and for stimulated wells it is negative.

The injectivity index, II, is often used as a rough estimate of the connectivity of the well to the surrounding reservoir. Mathematically, injectivity is defined as the change in the injection flow divided by the change in the stabilized reservoir pressure and its unit is [(L/s)/bar].

Wellbore storage, C, is defined as the difference between the wellhead flow rate and the sand face flow rate (i.e. the flow into or out of the actual formation). Wellbore storage effects can occur in several ways, but most commonly by changing the liquid level and fluid expansion. In injection testing the most dominant cause for wellbore storage is changing liquid level.

The radius of investigation, r_e is the approximate distance at which the pressure response from the well becomes undetectable, although the value of the parameter should be viewed more qualitatively.

Statistical parameters, e.g. the coefficient of variation CV, are defined as the ratio between the standard deviation σ and the mean value μ for the particular parameter in the model. The lower the value of *CV* the better is the modelling.

3.3 Injection well tests in Aluto-Langano

Injection step tests from LA-3 and LA-10D were simulated. Recordings were scarce from the test in LA-3 which was done in the 1980's but abundant from LA-10D which was done recently in a technically much better way. Yet it was possible to simulate the data from both of the wells with WT with some extra data manipulation. Tables 2 and 3 show the selected initial parameters and the selected model for the Welltester analysis of the injection tests of both wells.

TABLE 2: Initial parameters used in the well test analysis of LA-3 and LA-10D where those marked with * and are inserted by the user as well as the type of rock.

Parameters and units	LA-3	LA-10D
Estimated reservoir temperature [°C] *	300	300
Estimated reservoir pressure [bar-g]	97	91.45
Wellbore radius r [m] *	0.11	0.11
Porosity φ *	0.1	0.1
Dynamic viscosity of reservoir fluid μ, [Pa.s]	8.962×10^{-5}	8.6×10^{-5}
Compressibility of reservoir fluid c_w, [Pa^{-1}]	2.4413×10^{-9}	3.14×10^{-9}
Compressibility of rock matrix c_r, [Pa^{-1}]	2.44×10^{-11}	2.44×10^{-11}
Total compressibility C_t, [Pa^{-1}]	2.66×10^{-10}	3.36×10^{-10}

TABLE 3: Model selected for injection tests in wells LA-3 and LA-10D

Reservoir	Homogeneous
Boundary	Constant pressure
Well	Constant skin
Wellbore	Wellbore storage

3.4 LA-3

The third deep exploration well of the Aluto-Langano geothermal field, LA-3 was drilled between 21 January and 13 June 1983. The well was completed at 2143.9 m and the maximum measured temperature was 309°C at 1834 m after 132 hrs of warm up period. Loss of circulation encountered up to 10.5 L/s below 1890 m and complete loss of up to 29.2 L/s occurred between 2117 and 2143.9 m (Bödvarsson, 1986). The injection test in LA-3, consisted of three injection steps (9.7, 19.7 and 28.2 L/s) with increasing injection rates, followed by a falloff period as step no. 4. In Bödvarsson's report (1986), Figure 5 shows the injection/falloff data in a graph for well LA-3 (ELC, 1986). More points where added to injection steps of Figure 5 by reading off the graph because it was not possible to simulate the well with what was provided numerically for this project and clearly this had been done previously.

The reservoir parameters for all steps are shown in Table 4 and step four (the fall-off step) was selected as the best model, having lower CV values (Júlíusson et al., 2008) than the other steps. Clearly the modelling of step nr. 2 does not show good results with high CV in general. There the skin factor is positive but negative between -2.3 and -3.2 in the other steps so the closest surroundings of the well have higher permeability than the reservoir, having the effect that well acts as if its radius is larger than the real radius. The transmissivity is rather low and the storativity is relatively good. Figure 6 shows the results of the analysis of pressure against time in logarithmic scale (A) and log-log scale (B) for step 4 in the injection test. The log-log scale graph of pressure and time shows the derivative of pressure response multiplied by the time passed since the beginning of the steps. Derivative plots are helpful in determining the best reservoir model. As we can see from Figure 6 the model fits the collected data fairly well.

TABLE 4: Reservoir parameters from nonlinear regression model for well LA-3

Parameter	Step 1	CV %	Step 2	CV %	Step 3	CV %	Step 4	CV %
Transmissivity T (m^3/(Pa.s))	2.7×10^{-9}	5.5	1.1×10^{-8}	35.2	2.8×10^{-9}	14.9	5.7×10^{-9}	0.4
Storativity S ($m^3/(m^2Pa)$)	7.6×10^{-8}	3.4	1×10^{-8}	381.8	6×10^{-8}	12.8	5.5×10^{-8}	1.2
Radius of investigation r_e (m)	10	3	10	319.3	17	13.6	104	2.7
Skin factor s	-2.9	-	3	-	-3.2	-	-2.3	-
Wellbore storage C (m^3/Pa)	3.1×10^{-6}	1.7	5.7×10^{-6}	1.9	2.5×10^{-6}	11.4	4.8×10^{-6}	0.5
Reservoir thickness h (m)	284		23		227		206	
Permeability k (m^2)	9×10^{-16}		4.3×10^{-14}		1.1×10^{-15}		2.5×10^{-15}	
Injectivity index II ((L/s)/bar)	1.1		1.0		1		1	
Porosity φ	0.1		0.1		0.1		0.1	

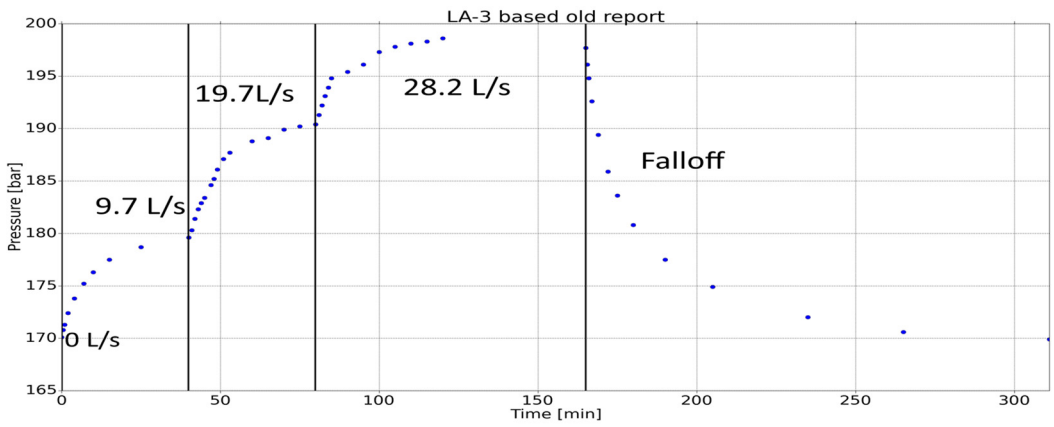

FIGURE 5: LA-3 pressure response and injection rate as a functionc of time in four injection steps with a total duration of 5.2 hours (based on data in ELC, 1986)

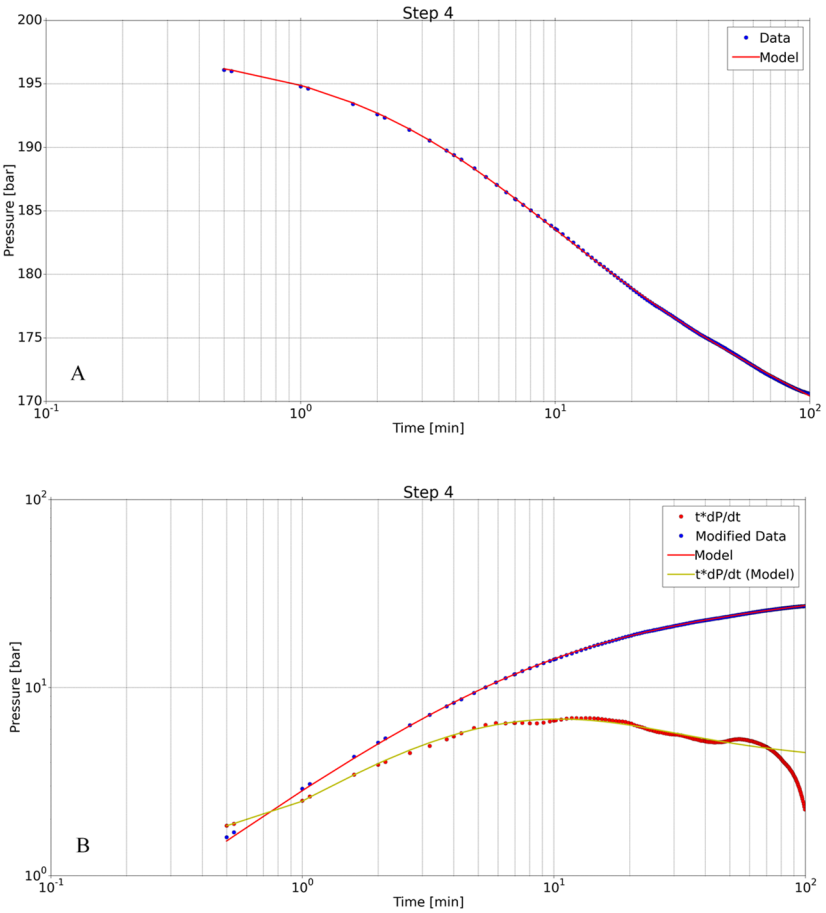

FIGURE 6: LA-3 model results and recorded pressure for step 4 using a logarithmic time scale (A) and log-log scale including the derivative (t*dp/dt) (B)

3.5 LA-10D

This is the second directional well drilled in Aluto-Langano geothermal project. It is the 10th deep well and was completed in October 2015. The well is drilled to the maximum measured depth of 1940 m in the direction of N43°W with an inclination of 28° and with a maximum measured temperature of 310°C at the bottom of well. The directional drilling kick off point (KOP) is at 450 m depth. The pressure temperature spinner (PTS) tool was set at 551 m depth and the water injection rate increased from 0 L/s to 14.9 L/s. After that, the injection rate was increased to 17, 19.3 and 21.7 L/s in the following steps and the pressure in the well was recorded (Figure 7). The injection rate of each step was stable for one hour.

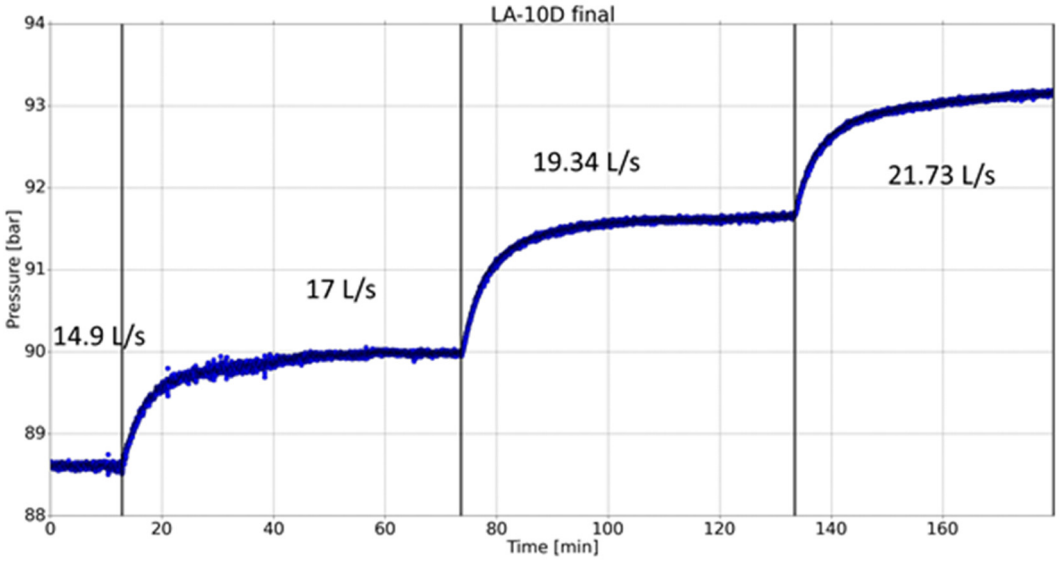

FIGURE 7: LA-10D pressure response and injection rate as a function of time in three injection steps with a total duration of 3 hours

The resulting reservoir parameters from the model for all steps are shown in Table 5 and the results of step three were selected as the best ones, having lower CV values than the other steps (Júlíusson et al., 2008). The results show relatively good transmissivity and storativity but the skin factor is not so good.

TABLE 5: Reservoir parameters from nonlinear regression model for well LA-10D

Parameter	Step 1	CV %	Step 2	CV %	Step 3	CV%
Transmissivity T (m^3/(Pa.s))	1.3×10^{-8}	0.7	2×10^{-8}	0.7	1.3×10^{-8}	0.4
Storativity S ($m^3/(m^2Pa)$)	5.1×10^{-8}	2.2	3×10^{-8}	3.4	5.7×10^{-8}	2.1
Radius of investigation r_e (m)	122	5.6	62	2.4	119	4.8
Skin factor s	0.07	-	3.1	-	-0.3	-
Wellbore storage C (m^3/Pa)	3.1×10^{-6}	0.68	4.1×10^{-6}	0.24	4.3×10^{-6}	0.3
Reservoir thickness h (m)	152		87		168	
Permeability k (m^2)	7.1×10^{-15}		1.9×10^{-14}		6.8×10^{-15}	
Injectivity index II ((l/s)/bar)	1.4		1.4		1.6	
Porosity φ	0.1		0.1		0.1	

Figure 8 shows the result of the analysis of pressure as a function of time on logarithmic scale (A) and log-log scale (B). The log-log scale graph of pressure and time shows the derivative of pressure response multiplied by the time passed since the beginning of the steps. Derivative plots are helpful for determining the best reservoir model. As we can see from the Figure 8 the model fits fairly well the collected data.

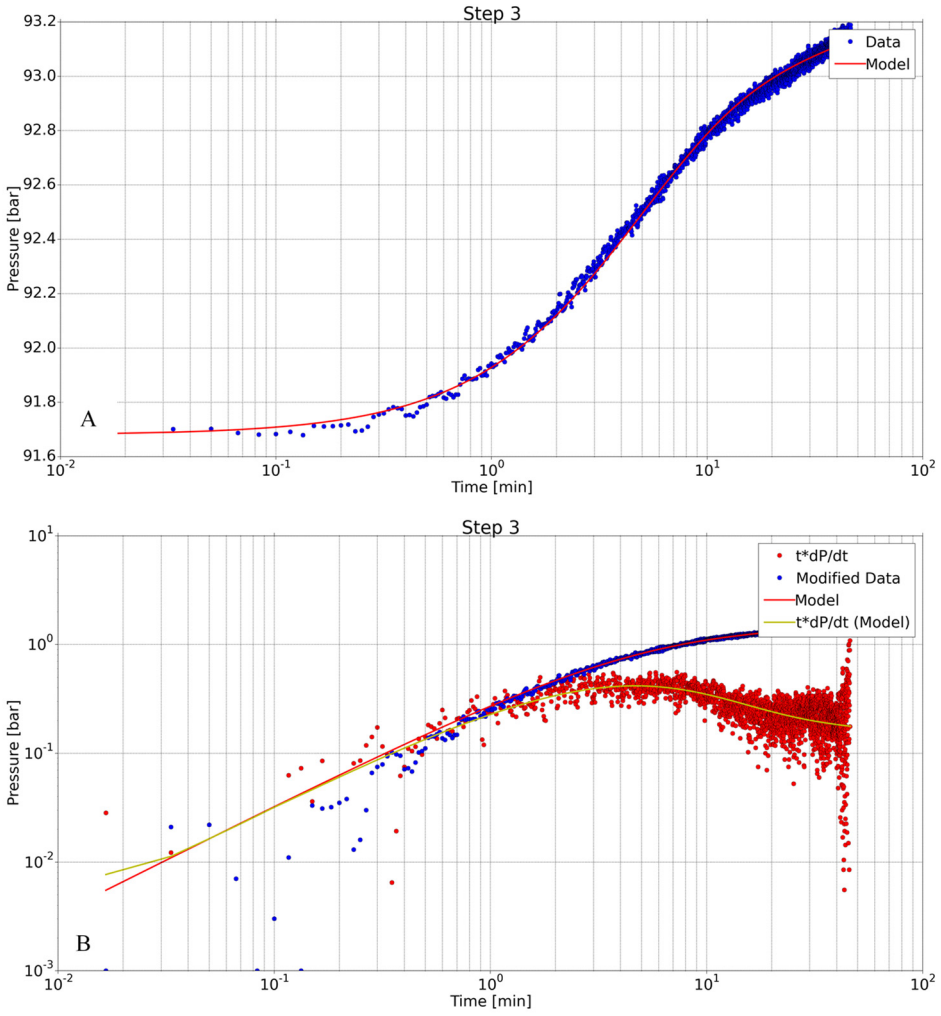

FIGURE 8: LA-10D model results and recorded pressure for step 3 using a logarithmic time scale (A) and log-log scale including the derivative (t*dp/dt) (B)

3.5.1 Modelling of step 3

Injection well test analyses done for wells LA-3 and LA-10D gave the best result for step number 4 and 3, respectively (Table 6) using a model assuming homogenous reservoir and constant boundary pressure. The skin factor values for the selected model steps are negative in both wells, which indicates that the nearest surroundings of the wells have higher permeability than the surrounding reservoir. The results (Tables 4 and 5) generally show better transmissivity in LA-10D than in well LA-3 and relatively good storativity as in LA-3. The skin factor on the other hand is not particularly good in LA-10D and not as good as in well LA-3.

TABLE 6: Estimated reservoir parameters of LA-3 and LA-10D from the best model and best step

Parameter	LA-3		LA-10D	
	Step 4	CV %	Step 3	CV %
Transmissivity, T (m^3/(Pa.s))	5.7×10^{-9}	0.4	1.3×10^{-8}	0.4
Storativity, S ($m^3/(m^2Pa)$)	5.5×10^{-8}	1.2	5.7×10^{-8}	2.1
Radius of investigation, r_e (m)	104	2.7	119	4.8
Skin factor, s	-2.3	-	-0.3	-
Wellbore storage, C (m^3/Pa)	4.8×10^{-6}	0.4	4.1×10^{-6}	0.3
Reservoir thickness, h (m)	206		168	
Permeability, k (m^2)	2.5×10^{-15}		6.8×10^{-15}	
Injectivity index, II ((L/s)/bar)	1.0		1.6	
Porosity, φ	0.1		0.1	

The injectivity indices are rather low in both of the wells, but higher in the new well LA-10D than in LA-3. Both wells LA-3 and LA-10D produce from a liquid-dominated reservoir.

4. ANALYSIS OF FORMATION TEMPERATURE AND INITIAL PRESSURE PROFILES

4.1 Introduction

Temperature and pressure logs are used extensively in geothermal exploration and development. The temperature and pressure logs are measured during drilling of wells, during heating up, after drilling and during flow tests as well as for monitoring. During drilling, the well temperatures are highly disturbed by drilling fluid circulations with cold water being injected into the well. During drilling the temperature logs provide valuable information on the location of aquifers (feed zones) and their relative sizes (permeability). Internal flow often exists in very permeable wells with multiple feed zones. This flow is clearly seen in temperature logs as constant temperature in the depth interval between feed points in the well, and sometimes the internal flow rate can be estimated based on temperature transients (Steingrímsson, 2013).

In geothermal investigation, temperature and pressure logging is important in determining formation temperature and reservoir pressures. The temperature and pressure disturbances that occur in a well during drilling will fade away gradually after the drilling stops. The wells will heat up and reach thermal equilibrium with the surroundings within several weeks or months and the well pressures will also recover after drilling and reach equilibrium with the permeable feed zones of the well. Temperature and pressure logs during the recovery period after drilling are the most important data to estimate formation temperatures and reservoir pressure (Steingrímsson, 2013).

Conditions inside the well during logging are not the same as in the surrounding formation or as undisturbed conditions in the reservoir before drilling. Different methods are used to estimate the formation temperature and pressure. Formation temperature can be estimated by extrapolation of a short

term temperature data from the well logs during warm up at selected depth for each estimation using Horner plot method (Steingrímsson, 2013).

The Horner plot method is a simple analytical technique used for analysing temperatures to determine the formation temperature (Helgason, 1993). The basic criterion for the technique is the linear relationship between measurements of temperatures at the selected depth and ln(τ):

$$\tau = \frac{\Delta t}{\Delta t + t_0} \tag{5}$$

where τ = Horner time;
Δt = Time passed since circulation stopped (s);
t_0 = Circulation time (s).

By using the equation above one can plot the wellbore temperature at the selected depth from logs during the warm up as a function of ln(τ) and then plot a straight line through the data. Extrapolation to ln(τ) = 0 gives an estimate of the formation temperature (Helgason, 1993). A computer software from the ICEBOX package, BERGHITI, is used for estimation of formation temperatures (Arason et al., 2004; Marteinsson, personal communication).

The reservoir pressure is estimated from data obtained during the recovery period. It is determined with the help of another software called PREDYP from ICEBOX (Arason et al., 2004) using the obtained formation temperature as a function of vertical depth and known initial wellhead pressure or water level as input. The warm up pressure profiles are plotted to determine their intersection with each other, known as pivot point, which shows the depth and pressure at the best zone in the borehole and can be considered as the actual pressure value in the reservoir. The water level is changed in PREDYP until the pressure at the depth of the pivot point matches the pressure in the logs.

In Sections 4.2 and 4.3, the temperature and pressure profiles are analysed to determine the formation temperatures and estimate the initial reservoir pressure for Aluto-Langano wells LA-9D and LA-10D. The temperature and pressure measurements in these wells were performed during injection and warm up of the wells, but only logs during warm up can be utilized to find the formation temperature. Figure 9 shows an example of results from BERGHITI.

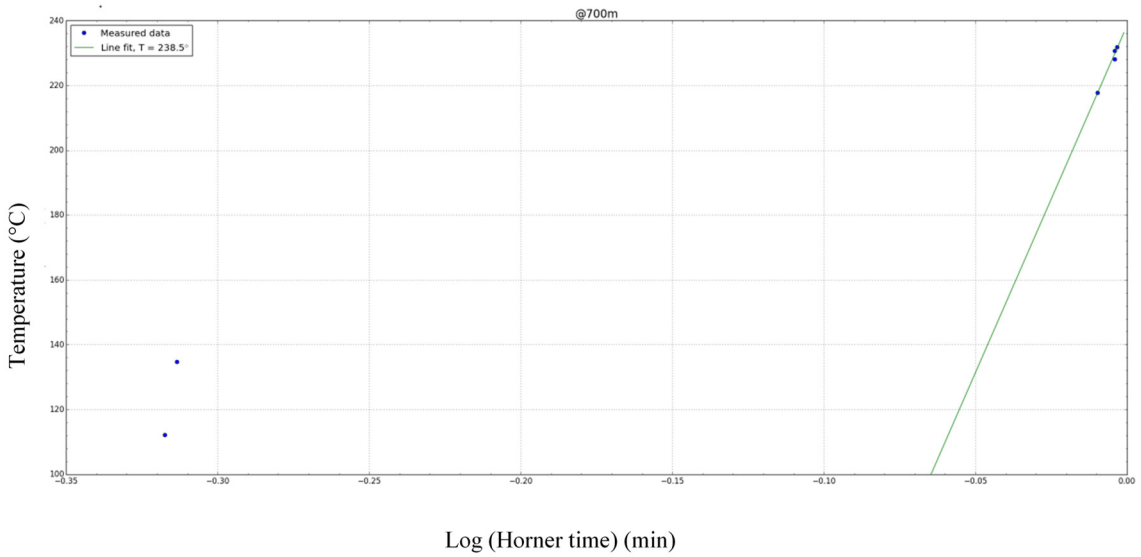

FIGURE 9: Formation temperature at 700 m in well LA-9D estimated with the Horner method

4.2 Well LA-9D

Drilling of well LA-9D started on November 12, 2013. Drilling of this well was interrupted due to repeated loss of circulation and insufficient water supply system to continue drilling blind. After procurement of water supply pumps and equipment, drilling was re-started on February 1, 2015 and was completed on April 30, 2015. The directional drilling kick off (KOP) is at 700 m where the well turns to a direction of N70°W with 51° maximum inclinations. Table 7 shows its depths and casing depths.

TABLE 7: Depths and casing depths in LA-9D with respect to ground surface and casings information

Depth (m)	Vertical depth (m)	Bit size (")	Casing diameter (")	Casing depth (m) from ground surface
60	60	26	20	56.7
210	210	17 ½	13⅜	207.9
608	608	12 ¼	9⅝	605
1920	1785	8 ½	7	1915

In well LA-9D seven small feed zones were located at 760, 830, 940, 1000, 1136, 1585 and 1707 m vertical depth, while a large feed zone was encountered at 1333 m vertical depth. The feed zones were identified from logs during injection and warm up logs and with the help of loss of circulation data sets.

The water injection into the well was stopped at 00:00 on 7 May 2015 and the temperature recovery was monitored. The logging during the warm up period was done with a PTS (pressure, temperature, spinner) tool on the 7th, 8th and 9th of May. Additional measurements were carried out on 1 of June to check the well temperature conditions and PTS measurements were carried out on 5 May. However, due to problems at the spinner part of the tool, only pressure and temperature were obtained (WJEC, 2015).

The temperature recovered steadily and the temperature below 1870 m depth exceeded 250°C during the log on 7 May. The logging survey on 9 May recorded more than 280°C around the well bottom of about 1900 m depth. On 1 June the temperature had recovered slightly more than during the first warm up logs. Focusing on the production zone of the well, the measured temperature is 192°C, at casing shoe (605 m) and 306°C at the maximum logging depth (1911 m) in the log from 1st June (Figure 10).

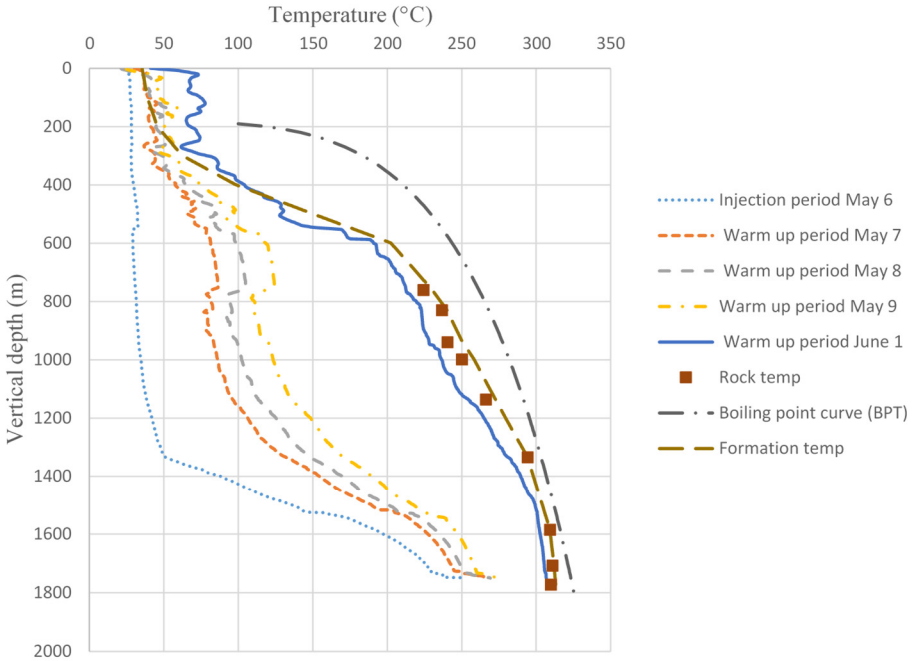

FIGURE 10: Temperature logs with injection, during warm up, boiling point curve (BPT) and estimated formation temperature of LA-9D

The formation temperature was estimated from the data set obtained during the temperature recovery of the well. The estimated formation temperature increases with depth and reaches about 309°C at the well bottom. The data points to be used in the BERGHITI program were selected from the temperature logs at the depth of the feed zones, their estimated formation temperatures were determined and then plotted in Figure 10 with the temperature logs as a function of vertical depth. The formation temperature of the well was estimated from these points. The formation temperature increases with depth in the production part of the well to 300-311°C.

To calculate the initial pressure, the estimated formation temperature profile from Figure 10 was used as input to the PREDYP program. The water level was adjusted in the calculations until the calculated profile matched the pivot point pressure. The pressure match was achieved with water levels at approximately 200 m vertical depth. The pressure profile obtained during the warm up period and the initial pressure profile are shown in Figure 11 as a function of vertical depth. The pivot point of LA-9D is located at 1100 m vertical depth where pressure of 85 bar has been measured in the 4 relevant logs.

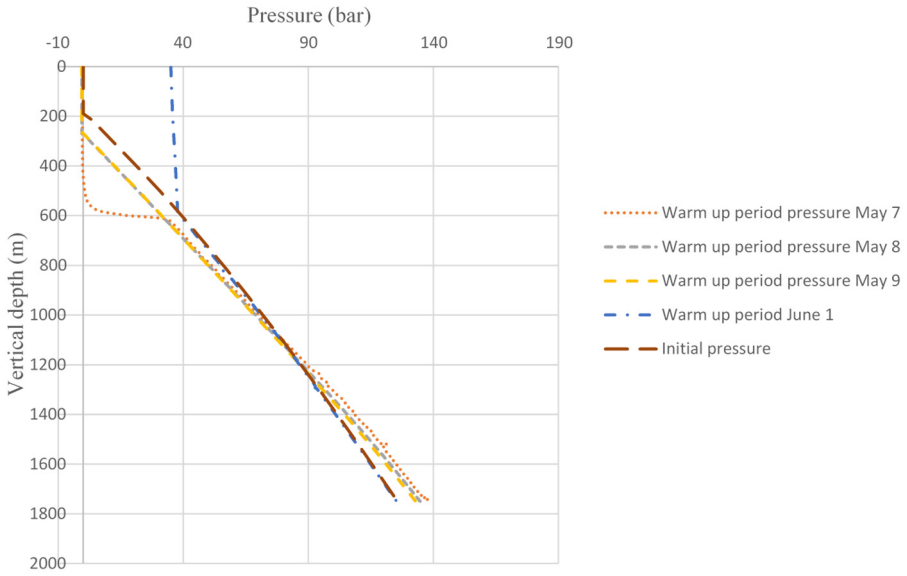

FIGURE 11: Pressure logs during warm up period and estimated initial pressure of LA-9D

4.3 Well LA-10D

Drilling of well LA-10D started on 25 June, 2015 and was completed on 2 October, 2015. The directional drilling kick off point (KOP) is at 450 m depth where it turns to a direction of N43°W with a maximum inclination of 28°. Table 8 shows its depths and casing depths.

In well LA-10D six small feed zones were located at 909, 1244, 1260, 1519 and 1642 m, vertical depth, while a large feed zone had been encountered at 699 m vertical depth (circulation loss zone).

The water injection into the well was stopped at 00:00 on 5 October 2015 and the temperature recovery was monitored. The monitoring logs were carried out after 12 hours and 24 hours, on October 6 and on October 24, 2015. Additional measurements were carried out on 18 November and 19 November 2015 to check the well temperature conditions but are not used in this study since the data recovered were of very poor quality.

The temperature recovered steadily and the temperature below 1700 m depth exceeded 250°C in the first log after 6 hours warm up. In the logging survey on 24 October, temperatures of more than 300°C were recorded around the well bottom at about 1800 m depth. Focusing on the production zone of the

well, the measured temperature is more than 200°C at casing shoe depth (807 m) and more than 300°C at maximum logging depth (1800 m) (Figure 12).

The formation temperature was estimated from the temperature well logs during warm up on 6 and 24 October (12 hours and 24 hours), respectively. Frequent temperature logging during warm up is strongly advised since too few temperature logs from that period increase the uncertainty of the estimated formation temperature. The estimated formation temperature increases with depth and reaches about 305°C at the well bottom at 1800 m depth (Figure 12).

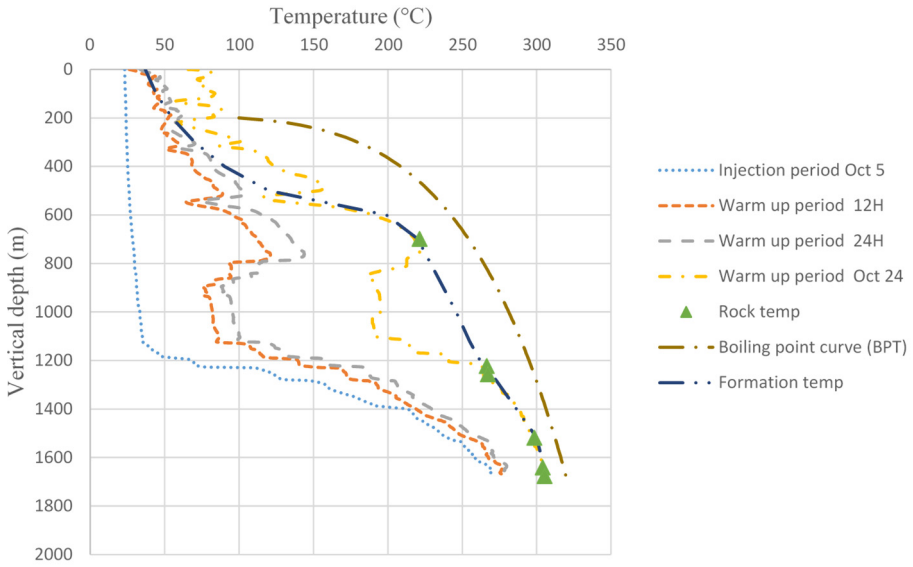

FIGURE 12: Temperature logs with injection, during warm up, boiling point curve (BPT) and estimated formation temperature of LA-10D

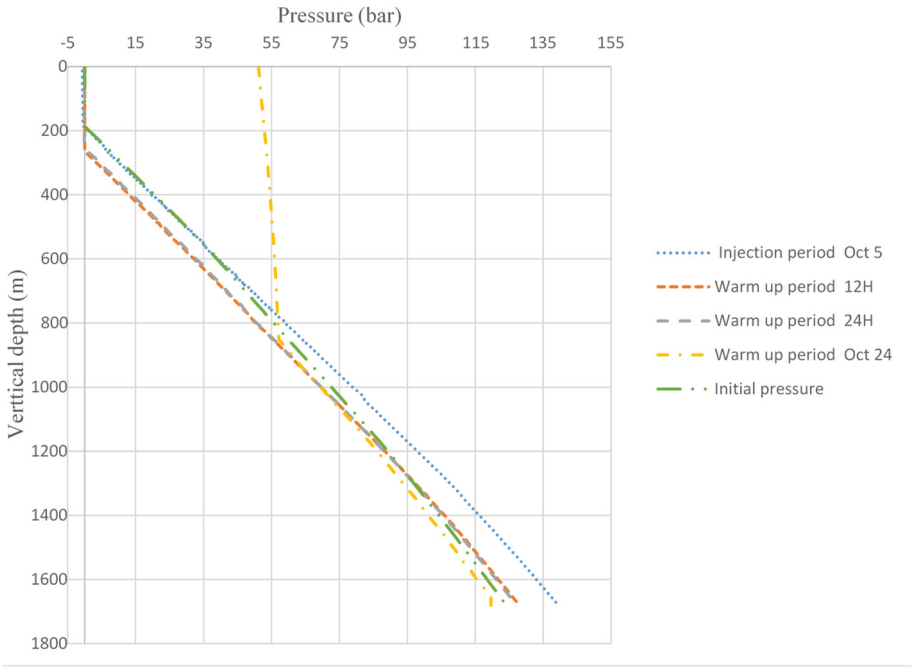

FIGURE 13: Pressure logs during warm up period and estimated initial pressure of LA-10D

The data points to be used in the Berghiti program were selected from the temperature logs at the depth of selected feed zones. Their estimated formation temperature was determined and plotted with the well logs in Figure 12 as a function of vertical depth.

The pivot point of LA-10D is located at 1200 m vertical depth where pressures of 92 bar where measured. To calculate the initial pressure, the estimated formation temperature profile from Figure 12 was used as input to the PREDYP program. The water level was adjusted in the calculations until the calculated profile matched the pivot point pressure. The pressure match was achieved with water levels at approximately 200 m depth. The pressure profiles obtained during the warm up period and the initial pressure profile are shown in Figure 13 as a function of vertical depth.

5. DISCHARGE TESTING

5.1 Introduction

Discharge testing is performed after a well has been allowed to warm up and recover its temperature. As the temperature of the fluid increases during the warm up period, in a high temperature geothermal field wellhead pressure sometimes builds up. The first step in flow testing is starting the well discharge. For most wells this is not difficult, since they naturally develop sufficient pressure, either cold gas or steam, so that opening the control valve will initiate flow. But in some wells it can be difficult to start fluid flow. Even after waiting for weeks for the well to heat up, no pressure develops at the wellhead, and when the valve is opened there is no flow. This is most common in wellbores that have cold sections in the upper part of the well (Grant and Bixley, 2011). Different methods like gas lift, steam injection and work overs are used to stimulate geothermal wells.

During the warm-up period, the water level in the well will gradually rise and eventually build a wellhead pressure above atmospheric pressure if the well is artesian. When the wellhead pressure has built up sufficiently, a discharge test can be conducted by flowing the well through an orifice (Bödvarsson and Witherspoon, 1989). Measurements can be performed to evaluate the total flow rate and enthalpy of the fluid. The lip pressure method (James, 1970) or often called Russel James method, can be used to determine the total flow rate and enthalpy with a simple weir being used to measure liquid flow. By repeating these flow tests with different sized orifices, the well productivity as a function of wellhead pressure can be determined. That is one of the so called characteristic curves for the well that can be used in selecting operating conditions for the turbines in the power plant (Bödvarsson and Witherspoon, 1989).

If environmental conditions permit, a short term discharge test can be used applying the lip pressure method to get a first estimate of the longer term production potential and to determine the most suitable equipment for longer term testing. The discharge can also help to clear debris from the well (Grant and Bixely, 2011). Russel James lip pressure method is used to determine the flow characteristics and production capacity of both wells LA-9D and LA-10D during discharge testing.

5.2 Russel James lip pressure method

The lip pressure method is a convenient means of measuring the flow of many geothermal wells. It is based on an empirical equation developed by Russell James (1970) and is considered to be the most versatile method for testing all medium-enthalpy wells. Grant and Bixely (2011) stated: ‘‘To use this method, the steam-water mixture is discharged through an appropriately sized pipe into a silencer or some other device to separate the steam and water phases at atmospheric pressure (Figure 14). The lip pressure is measured at the extreme end of the discharge pipe using a liquid-filled gauge to damp out pressure fluctuations. Water flow from the silencer is measured using a sharp-edged weir near the silencer outlet.’’

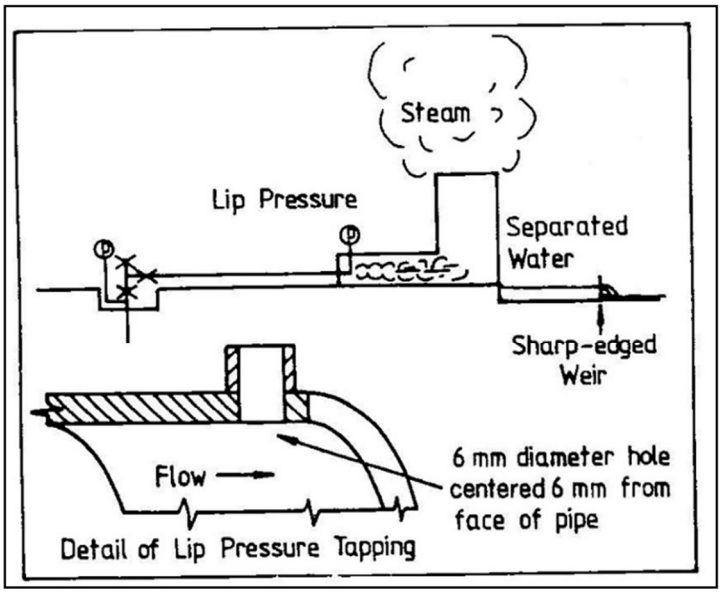

FIGURE 14: Flow measurement by lip pressure and silencer (Grant et al., 1982)

Grant and Bixely (2011) said: ‘‘James’s formula, relates mass flow, discharge pipe area, enthalpy, and lip pressure”. The empirical formula can be presented as:

$$Q = \frac{184\, p_{lip}^{0.96} A}{H_t^{1.102}} \tag{6}$$

where Q = Total flow rate (kg/s);
P_{lip} = Lip pressure (bar-a);
A = Cross-sectional area of the discharge pipe (cm^2); and
H_t = Total enthalpy (kJ/kg).

According to Grant and Bixeley (2011) Equation 7 is used when the flow is measured in tonnes per hour.

$$Q = \frac{663 p_{lip}^{0.96} A}{H_t^{1.102}} \tag{7}$$

The total mass flow rate obtained from Russel James lip pressure method can be related to water flow rate measured at the silencer after flashing:

$$Q = \frac{H_s - H_w}{H_s - H_t} Q_w \tag{8}$$

where Q_w = Water flow rate measured at the silencer after flashing (kg/s);
H_s & H_w = Saturated steam and saturated water enthalpies at the separation pressure measured in kJ/kg.

If we combine Equations 6 and 8 we obtain:

$$\frac{Q_w}{AP^{0.96}} = \frac{184}{H^{1.102}} \frac{H_s - H_t}{H_s - H_\omega} \tag{9}$$

The steam mass fraction X can be calculated as:

$$X = \frac{H_t - H_w}{H_s - H_w} \tag{10}$$

By measuring the lip pressure, water flow rate and cross-sectional area of the pipe then the total enthalpy can be obtained numerically. The enthalpies of steam and water can be obtained with the help of steam tables from their corresponding temperatures and pressures.

With the help of the LIP program from the ICEBOX software package (Arason et al, 2004; Marteinsson, 2016), the enthalpies and flow rates are calculated considering weir properties corresponding to a standard 90° V-notch weir box.

5.3 Discharge testing of well LA-9D

Figure 15 shows recordings during two flow test in well LA-9D. The one-month long discharge test of well LA-9D was started on 4 November 2015 by opening the master valve and the discharged geothermal fluid was sent to a silencer. The mass flow data was measured every one hour during the testing period. The different sizes of discharge pipe with diameter of 3″, 4″, 5″ and 6″ were used to obtain the stable discharge mass flow data at different wellhead pressure. The lip pressure was monitored as well as the wellhead pressure (WHP) and the height of the liquid in the weir-box. Fluid sampling was also carried out for chemical analysis. The well was closed on 4 December 2015 to finish the one-month single-well discharge test (Table 9).

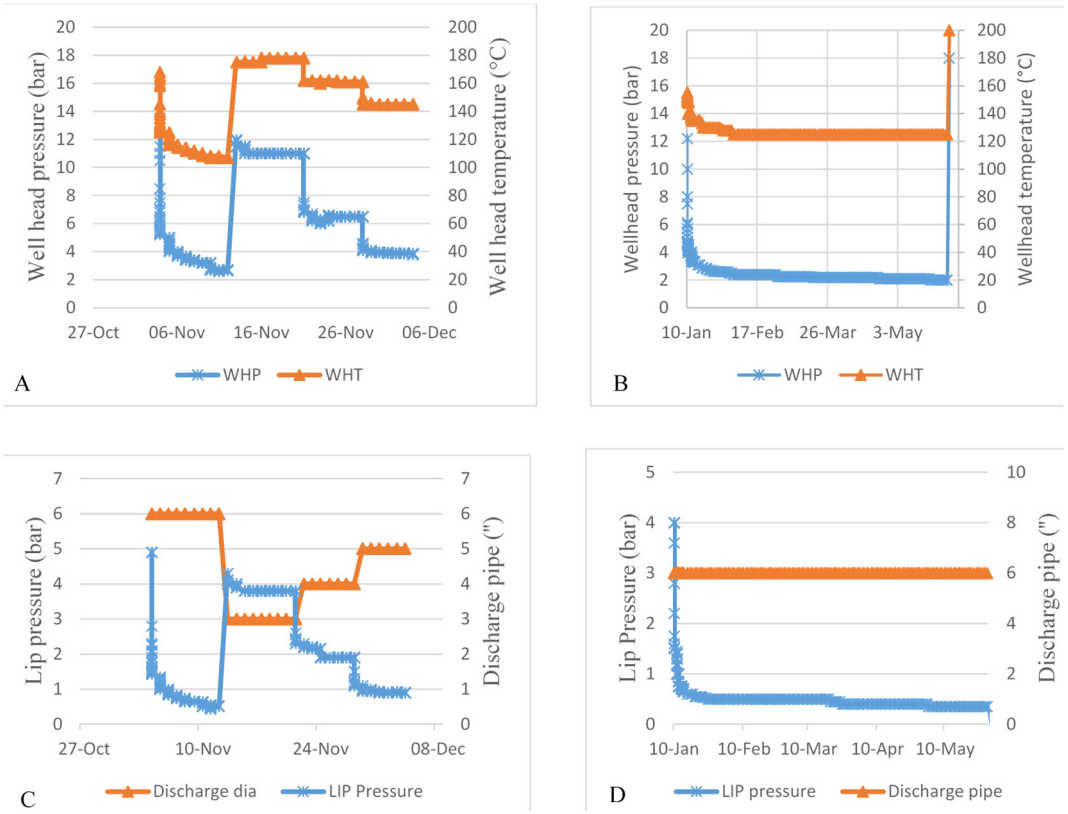

FIGURE 15: First (A and C) and second (B and D) discharge test data of well LA-9D, showing wellhead pressure and temperature (A and B), lip pressure and discharge pipe diameter (C and D)

Then well LA-9D was discharged again on 10 January 2016 (Table 9) which was during the period when well LA-10D was discharging continuously. The two wells were discharged simultaneously until well LA-10D was closed on 1 June 2016. The PTS logging (flowing survey) was carried out on 18 March 2016 to obtain the data on flow conditions in the wellbore. The master valve of LA-9D was closed gradually from 27 May and completely shut off on 1 June 2016. The fluid was discharged through a 6" discharge pipe and the wellhead pressure and the total mass flow rate was 2.25 bar-g and about 10.61 kg/s, respectively. Figure 15 shows wellhead temperature, wellhead pressure (A and B), lip pressure and discharge pipe (C and D) of the first and second discharge for well LA-9D.

TABLE 9: Measurements and results for well LA-9D from the Russel James lip pressure method with separation pressure of 1 bar-a

No.	Date	P_0 (bar)	P_c (bar)	D_p (")	W_{height} (cm)	H (kJ/kg)	Q_t (kg/s)	Q_w (kg/s)	Q_s (kg/s)	X
1	2015-11-12	2.7	0.5	6	8	2152.8	10.7	2.7	8	0.7
2	2015-11-20	11	3.8	3	8.5	1949.3	9	3.1	5.9	0.7
3	2015-11-27	6.5	1.9	4	8.3	2025.1	9.4	2.9	6.5	0.7
4	2015-12-04	3.8	0.9	5	8	2087.3	9.5	2.7	6.8	0.7
5	2016-05-27	2.3	0.5	6	8	2147.6	10.6	2.7	7.9	0.7

The calculated water, steam, total mass flow rate and fluid enthalpy of the first and second discharge test of LA-9D are shown in Figure 16. At the beginning of the test and at the time of discharge pipe replacement the flow rate is relatively higher but stabilizes with time, even stabilized flow rate data were obtained with different discharge pipe sizes.

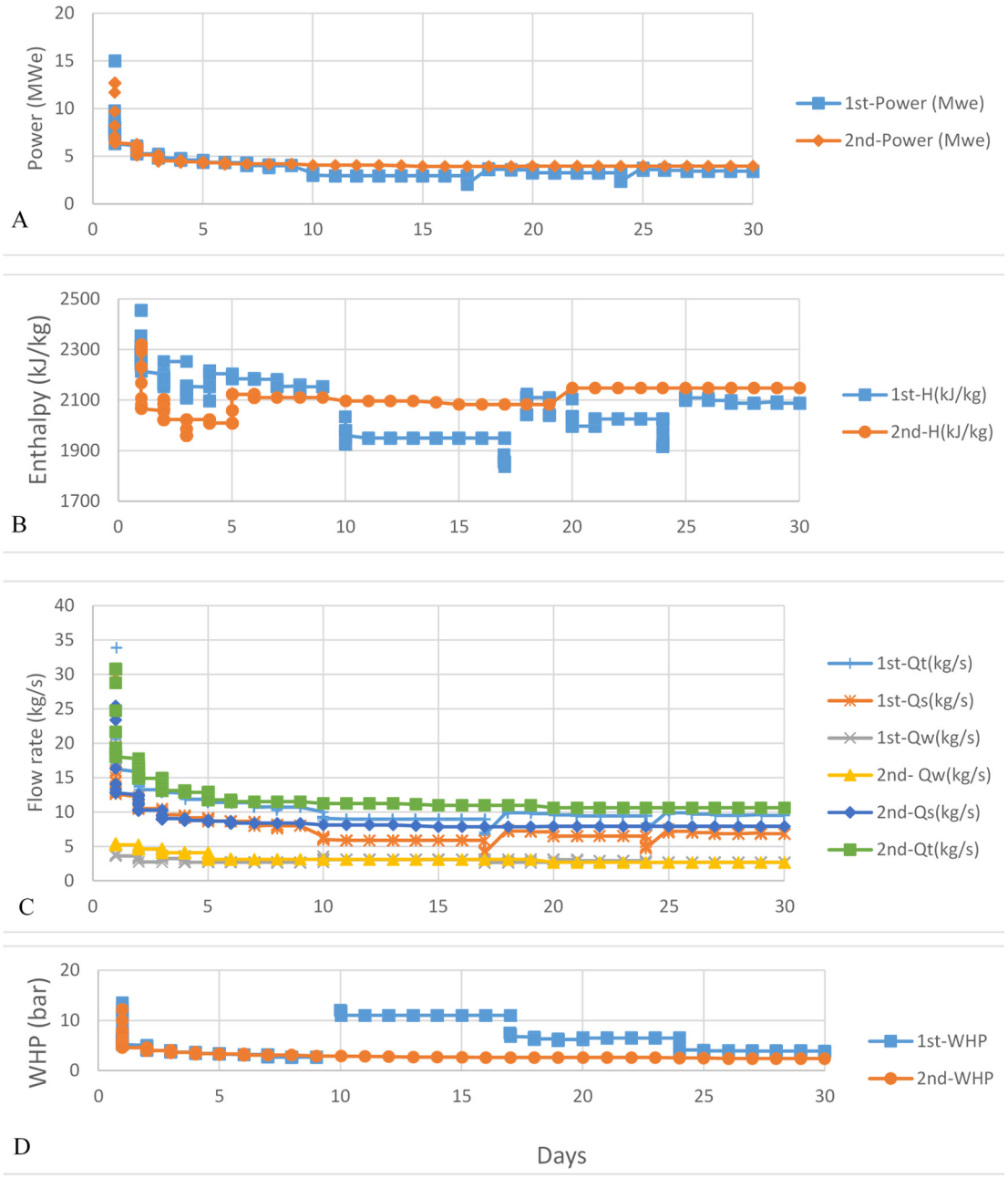

FIGURE 16: Results of the first 30 days of LA-9D long term discharge test, after which it was constant (see Figure 15 B and D), showing power (A); enthalpy (B); flow rate (C); and well head pressure (D in the two flow tests (1st and 2nd)

The analysis of the measurements from the single well discharge (first discharge) test of well LA-9D gives an estimate of steam flow in the range of 5.9-8.0 kg/s at the separation pressure of 1 bar-a (Table 9) which is equivalent to 2.4-5.6 MW of electric power output assuming 2 kg/s of steam flow convert to 1 MW_e. The steam flow rate at the wellhead of 6.5 bar-g was 6.49 kg/s which is equivalent to 3.2 MW_e. Table 10 shows the results with a separation pressure of 5 bar-a, as in the Aluto-Langano pilot power plant.

TABLE 10: Measurements and results for well LA-9D from Russel James lip pressure method with separation pressure of 5 bar-a, as in the Aluto-Langano pilot power plant

D_p (in)	Q_w (kg/s)	Q_s (kg/s)	X
6	3.1	7.6	0.6
3	3.5	5.5	0.4
4	3.3	6.1	0.5
5	3.1	6.5	0.5
6	3.1	7.5	0.6

5.3.1 Flow characteristics

Geothermal wells can be characterized by their mass flow and enthalpy of the steam-water mixture produced at various wellhead pressures. By plotting these characteristics, the general processes occurring in the reservoir can be inferred.

The well characteristic curves of LA-9D are shown in Figure 17, as entities of the relationship between wellhead pressure and steam, water, total mass flow rate and fluid enthalpy were extracted from the well. These were calculated and plotted using relatively stable data at different wellhead pressures. The wellhead pressure of LA-9D was 2.25 bar-g using the 6-inch discharge pipe. It rose up to 11 bar-g when the 3-inch discharge pipe was used. Enthalpy increases when wellhead pressure decreases, at 11 bar it is 1950 kJ/kg and reaches 2153 kJ/kg at 2.65 bar. The steam flow rate is around 5.9-8.0 kg/s for separation pressure of 1 bar but 5.5-7.6 kg/s with separation pressure of 5 bar. The steam flow rate at 11 bar is around 6 kg/s and 8 kg/s at 2.65 bar. The flow data show that the fluid enthalpy decreases when the wellhead pressure is lowered. This is rather unusual but suggests that the feed zones of the well produce fluid of different enthalpies and the contribution of the lower enthalpy feed zones becomes larger than that of the higher enthalpy feed zones when the wellhead pressure is lowered.

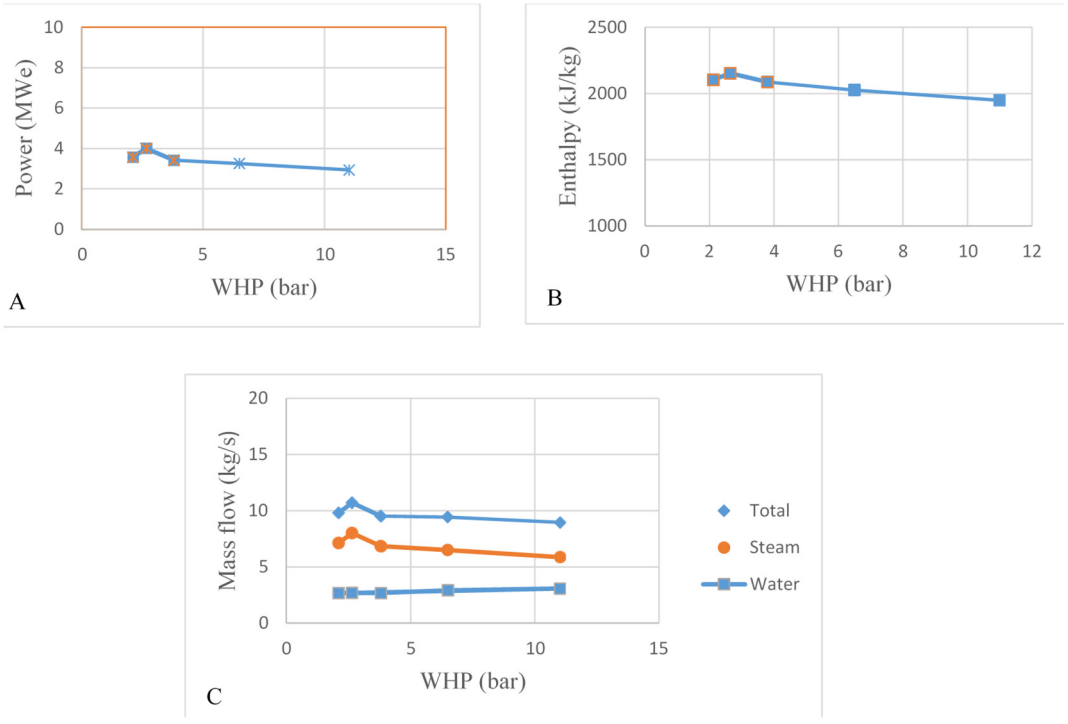

FIGURE 17: Characteristic curves of LA-9D showing power (A), enthalpy (B) and mass flow rate (C) as a function of well head pressure (WHP)

Figure 17 shows that the flow rate does not increase much when the wellhead pressure decreases. This behaviour is typical for two-phase wells where boiling starts in the formation and water and steam enter the well. The main pressure drop during flow occurs then in the formation, not in the well. Often a pressure drop >100-150 bar is seen in two-phase wells and 90% of the drop is before the two-phase fluid enters the well. A change in the wellhead pressure of 5-10 bar is then a realtively small change of the total drawdown and does not change the flow much. The flat section of a deliverability curve formation indicates formation controlled flow or formation choked flow. Steep deliverability curves, which are typical for single-phase liquid inflow wells, indicate that the wellbore is controlling the flow from the well.

5.4 Discharge testing of well LA-10D

Figure 18 shows measurements during two flow tests in well LA-10D. The first long term discharge test of LA-10D was started on 8 December 2015. The mass flow data was measured every one hour during the testing period. Different sizes of discharge pipe with diameter of 3″, 4″, 5″ and 6″ were used to obtain stable discharge mass flow data at different wellhead pressures. The single well discharge test of LA-10D was completed on 9 January 2016. The PTS logging was carried out on 21 March 2016 to obtain data on flow conditions in the wellbore. On 24 May, LA-10D was discharged again and the discharge was completed on 15 June 2016.

The PTS logging was attempted on 14 and 15 of March 2016 at LA-10D while the well was discharging though a 6″ discharge pipe. However, the tool could not go deeper than 1040 m and 1113 m, respectively. On 21 March 2016 the sinker bar (weight bar) was connected to the tool and then the tool could reach close the well bottom. The wellhead pressure was 3.25 bar-g and the total mass flow rate was 12.8 kg/s

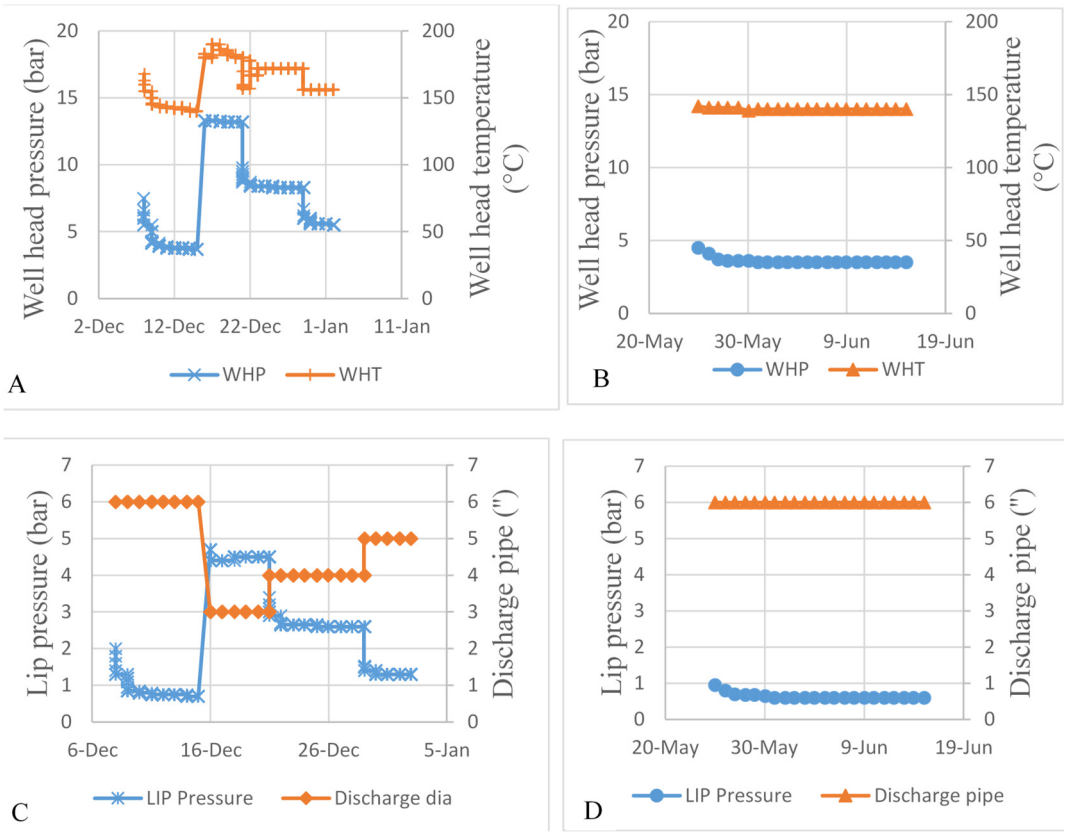

FIGURE 18: First (A and C) and second (B and D) discharge test data of well LA-10D, showing wellhead pressure and temperature (A and B); and lip pressure and discharge pipe diameter (C and D)

during the survey. The pressure, temperature, and spinner rotation data in the well were continuously measured and recorded from wellhead to close to the well bottom with the PTS tool.

The calculated water, steam, total mass flow rate and fluid enthalpy of the first and second discharge test of LA-10D are shown in Table 11 and Figure 19. The first month is the period of single well discharge test and the rest is the period of multi well discharge test together with well LA-9D. Different discharge pipe sizes were used in the test and almost stable flow rates at each condition were obtained.

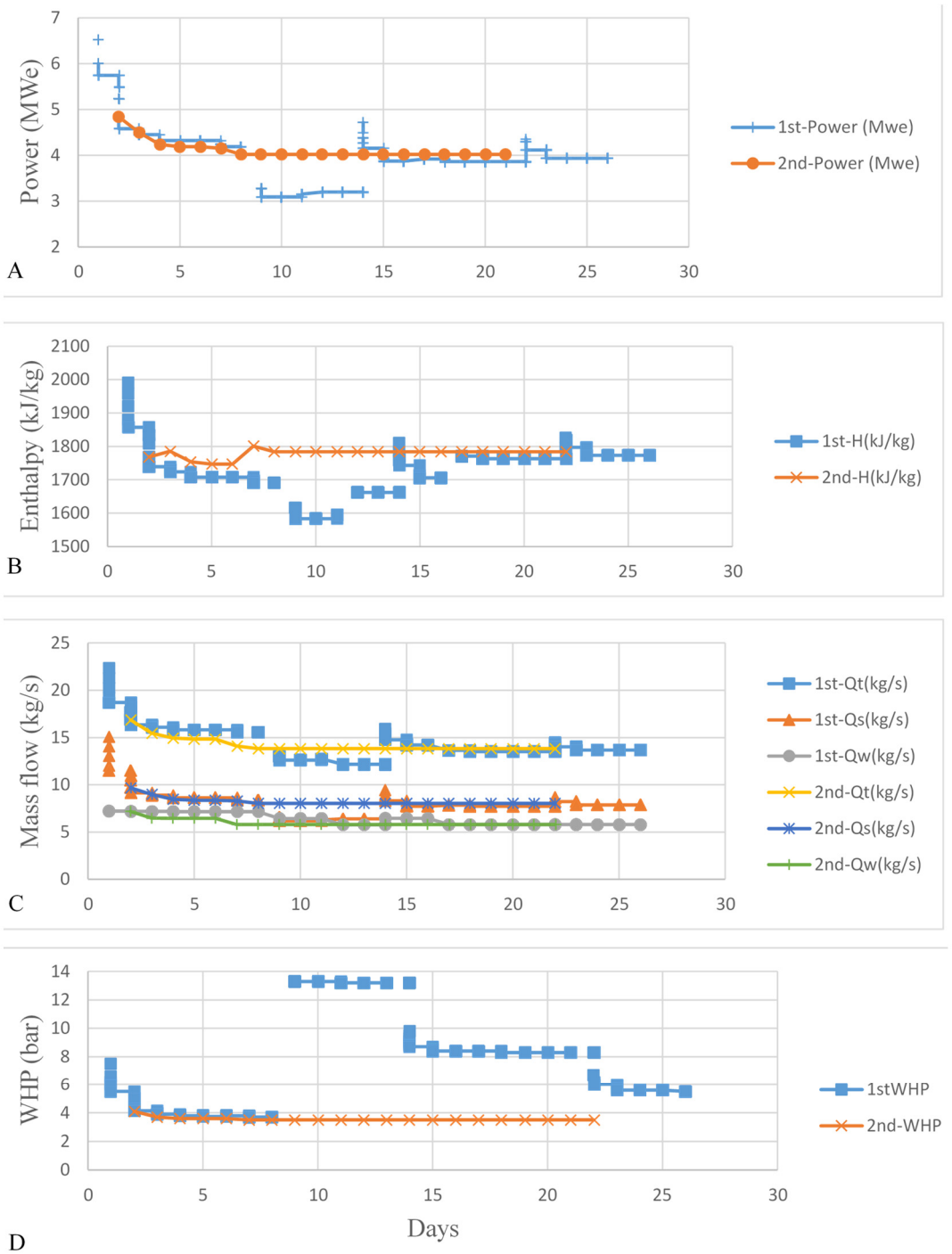

FIGURE 19: Results of first 30 days of LA-10D long term discharge test, after which it was constant (see Figure 18 B and D), showing power (A), enthalpy (B), flow rate (C), and well head pressure (D), and in two flow tests (1st and 2nd)

TABLE 11: Measurements and results for well LA-10D from the Russel James lip pressure method with separation pressure of 1 bar-a

No.	Date	P_0 (bar)	P_c (bar)	D_p (inch)	W_{height} (cm)	H (kJ/kg)	Q_t (kg/s)	Q_w (kg/s)	Q_s (kg/s)	X
1	2015-12-15	3.7	0.7	6	12	1691.3	15.6	7.2	8.4	0.6
2	2015-12-21	13.2	4.5	3	11	1662.2	12.2	5.8	6.4	0.6
3	2015-12-29	8.3	2.6	4	11	1763.1	13.5	5.8	7.7	0.6
4	2016-01-05	5.6	1.3	5	11	1773.6	13.7	5.8	7.9	0.6
5	2016-04-01	3.3	0.5	6	10.5	1815.1	12.8	5.8	7.6	0.6
6	2016-06-15	3.5	0.6	6	11	1784.3	13.8	5.8	8.1	0.6

The analysis of the measurements from the single well discharge test of well LA-10D gives an estimate of steam flow in the range of 6.4-8.4 kg/s at the separation pressure of 1 bar-a which is equivalent to 3.2-5.7 MW electric power assuming 2 kg/s of steam flow converts to 1 MW_e. The steam flow rate at the wellhead pressure of 8.3 bar-g is 7.74 kg/s and 7.87 kg/s at wellhead pressure of 5.6 bar-g. This is equivalent to 3.8-3.9 MW_e.

The 6-inch discharge pipe was used during the second test. The flow conditions became stable and the wellhead pressure and the total mass flow rate were constant at 3.5 bar-g and 13.83 kg/s. The steam flow rate and steam fraction are summarized in Table 12 and the equivalence of power (MW_e) for 5 bar-a separation pressure is in the range of 2.9-3.8 MWe.

TABLE 12: Measurements and results for well LA-10D from the Russel James lip pressure method with separation pressure of 5 bar-a as in the Aluto-Langano pilot power plant

D_p (″)	Q_w (kg/s)	Q_s (kg/s)	X
6	7.9	7.6	0.5
3	6.4	5.8	0.5
4	6.4	7.1	0.5
5	6.4	7.2	
6	5.8	7	
6	6.5	7.4	0.5

The well characteristic curves of LA-10D (Figure 20) shows the relationship between wellhead pressure and steam, water, total mass flow rate and fluid enthalpy extracted from the well, plotted using relatively

stable data at different wellhead pressures. The wellhead pressure of LA-10D was 3.25-3.7 bar-g while using the 6-inch discharge pipe. It rose up to 13.2 bar-g when the 3-inch discharge pipe was used. The steam flow rate is around 6-8 kg/s. The fluid enthalpy is 1662-1815 kJ/kg. The curves are relatively flat and the change of mass flow rate as a function of wellhead pressure is not large. At the end of the first long term discharge test, the wellhead pressure was 3.25 bar-g and the steam flow rate was 7.6 kg/s when using the 6″ discharge pipe. The stabilized wellhead pressure and steam flow rate were 3.5 bar-g and 8.1 kg/s, respectively, during the second discharge.

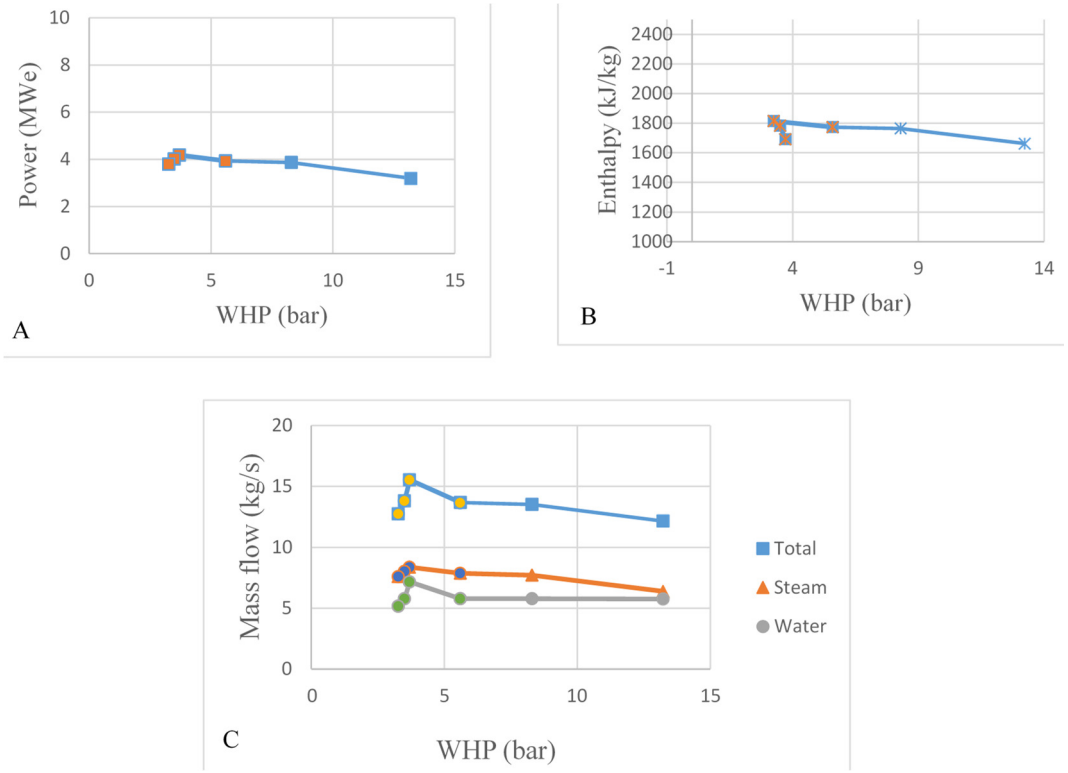

FIGURE 20: Characteristic curves of LA-10D showing power (A), enthalpy (B) and mass flow rate (C) as a function of well head pressure (WHP)

6. DISCUSSION AND CONCLUSION

The selected model for simulating the injection step tests in wells LA-3 and LA-10D assumed a homogenous reservoir and constant boundary pressure. The results show in general better transmissivity in LA-10D than in well LA-3 and a relatively good storativity in both of the wells. The transmissivity values were on the order of 10^{-9} [m^3/(Pa*s)] and 10^{-8} [m^3/(Pa*s)] for well LA-3 and LA-10D, respectively, and the storativity values in the order of 10^{-8} [m^3/(Pa*m^2) or m/Pa], the wells are classified as producers from a liquid-dominated geothermal reservoir.

The results for LA-3 for the skin factor for the best step show that it is -2.3 but in the range of -2.3 to -3.2 in the steps which had good simulations (CV criteria). These values indicate that the well has higher permeability in its closest surroundings than farther away and its effective radius is therefore larger than its real radius. The skin factor in the best step in LA-10D was on the other hand only -0.3 and in one step it was as high as 3.1, i.e. a positive skin factor, which means worse permeability in the close surroundings than farther away from the well.

The injectivity index is often used as a rough estimate of the connectivity of a well to the surrounding reservoir. Injectivity indices are fairly low for both wells with 1.1 (l/s/bar) for LA-3 and 1.6 (l/s/bar) for LA-10D.

Temperature and pressure data from LA-9D and LA-10D in the Aluto-Langano geothermal field were interpreted with the help of Horner plot method to estimate formation temperature. The corresponding initial pressure of the reservoir was found using the PREDYP in the ICEBOX software. Results from LA-9D and LA-10D show an estimated formation temperature ranging from 300 to 311°C and from 300 to 305°C, respectively, in the bottom of the wells. The pivot point of LA-9D is located at 1100 m vertical

depth with pressure of 85 bar. The pivot point of LA-10D is located at 1200 m vertical depth with pressure of 92 bar. The Horner plot method did not proof equally useful in the interpretation of LA-10D as it did in the interpretation of LA-9D. Only three warm up logs were available for LA-10D with the first two only 12 hours apart, making the results from the interpretation more uncertain than in the case of LA-9D.

The analysis of the measurements from the single well discharge (first discharge) test of well LA-9D gives an estimate of steam flow in the range of 5.4-7.6 kg/s at the separation pressure of 5 bar-a in Aluto-Langano pilot power plant which is equivalent to 2.7-3.8 MW_e of electric power output assuming that 2 kg/s of steam flow convert to 1 MWe.

The analysis of the measurements from the single well discharge test of well LA-10D gives an estimates of steam flow in the range of 5.8-7.6 kg/s at the separation pressure of 5 bar-a in Aluto-Langano pilot power plant which is equivalent to 2.9-3.8 MWe electric power assuming that 2 kg/s of steam flow convert to 1 MWe.

7. RECOMMENDATIONS

A major problem with the injection tests and all of the other injection tests performed on the Aluto-Langano wells lies in the test design. The time period for each of the steps is only about one hour. A better design could be to let each injection step last at least three hours. In cases where the water supply is a problem, it is preferable to reduce the number of injection steps rather than their duration. One or two steps of sufficient duration provide more useful results than ten steps that are too short. If the steps are long enough, they can all be analysed and produce good estimates.

It is important in new wells to measure temperature and pressure frequently during warm up, especially in the beginning of the warm up period for better interpretation of the formation temperature and initial pressure.

The importance of monitoring the wells through their lifetime should never be underestimated to be able to follow the evolution of the geothermal reservoir and the wells themselves.

ACKNOWLEDGMENTS

I want to express my deepest gratitude to the United Nations University, the Government of Iceland and the Ethiopian Electric Power (EEP) for allowing me to attend this training. I want to thank Mr. Lúdvik S. Georgsson, director of the UNU geothermal training program and Mr. Ingimar G.Haraldsson, deputy director for allowing me to study reservoir engineering, Ms. Thórhildur Ísberg, school manager, Mr. Markús A. G. Wilde, service manager and Ms. Málfrídur Ómarsdóttir, enviromental scientist and all staff of ÍSOR for the teachings and dedication to make us well educated.

My special thanks go to my supervisors, Dr. Svanbjörg H. Haraldsdóttir and Ms. Saeunn Halldórsdóttir, for sharing their great knowledge and experience, for their patience and support during this project as well as Mr. Benedikt Steingrímsson, for his valuable comments. I would also like to thank Mr. Kjartan Marteinsson for his support and guidance to the use of softwares developed at ÍSOR. Finally, I want to thank former geothermal project manager of EEP Mr. Mulugeta Asaye for believing in me and recommending me for studies in this study area.

Finally, I would like to thank my lovely wife Sofia Midaso for having Sena, my new born baby girl while I was doing this project.

REFERENCES

Arason, Th., Björnsson, G., Axelsson, G., Bjarnason, J.Ö., and Helgason, P., 2004: *The geothermal reservoir engineering software package ICEBOX, user's manual*. Iceland GeoSurvey - ÍSOR, Reykjavík, report ISOR-2004/014, 80 pp.

Axelsson, G., 2012: The physics of geothermal energy. In: Saying, A., (ed.), *Comprehensive Renewable Energy, 7,* 3-50.

Axelsson, G., 2013: Geothermal well testing. *Paper presented at "Short Course V on Conceptual Modelling of Geothermal Systems"*, *UNU-GTP and LaGeo, Santa Tecla, El Salvador*, UNU-GTP, SC-17, 30 pp.

Bödvarsson, G.S., and Witherspoon, P.A., 1989: Geothermal reservoir engineering, part 1. *Geotherm. Scie & Tech, 2-1,* 1-68.

Bödvarsson, G.S., 1986: *Independent review of reservoir engineering work at the Aluto-Langano geothermal field, Ethiopia*. Lawrence Berkeley Lab., US, for UN Department of Technological Cooperation for Development, NY, 59 pp.

ELC, 1986: *Exploitation of Langano-Aluto geothermal resources, feasibility report*. Electroconsult – ELC, Milan Italy, report.

Grant, M.A., and Bixley, P.F., 2011: *Geothermal reservoir engineering* (2nd ed.). Academic Press, Burlington, USA, 359 pp.

Grant, M.A., Donaldson, I.G., and Bixley, P.F., 1982: *Geothermal reservoir engineering*. Academic Press, NY, 369 pp.

Haraldsdóttir S.H., 2016: *Well testing theory - injection.* UNU-GTP Iceland, unpublished lecture notes.

Helgason, P., 1993: Step by step guide to BERGHITI. User's guide. In: Arason, Th., Björnsson, G., Axelsson, G., Bjarnason, J.Ö., and Helgason, P., 2004: *ICEBOX – Geothermal reservoir engineering software for Windows, a user's manual*. Iceland GeoSurvey - ÍSOR, Reykjavík, report ISOR-2004/014, 80 pp.

Horne, R.N., 1995: *Modern well test analysis, a computer aided approach* (2nd ed.). Petroway Inc., USA, 257 pp.

Hutchison, W., Mather, T.A., Pyle, D.M., Biggs, J., and Yirgu, G., 2015: Structural controls on fluid pathways in an active rift system: a case study of the Aluto volcanic complex. *Geosphere, 11-3,* 542-562.

James R., 1970: Factors controlling borehole performance. *Geothermics, Sp. issue, 2-2,* 1502-1515.

Júlíusson, E., Grétarsson, G.J., and Jónsson, P., 2008: *WellTester 1.0b, user's guide.* Iceland GeoSurvey - ÍSOR, Reykjavík, 27 pp.

Kebede, S., 2012: Geothermal exploration and development in Ethiopia: Status and future plan. *Paper presented at "Short Course VII on Exploration for Geothermal Resources", organized by UNU-GTP, KenGen and GDC, in Naivasha, Kenya*, UNU-GTP SC-15, 16 pp.

Marteinsson, K., 2016: *Well Tester User Manual. Version 2*. ÍSOR-. – Iceland GeoSurvey, Reykjavik, report in publication.

Steingrímsson, B., 2013: Geothermal well logging: Temperature and pressure logs. *Paper presented at "Short Course V on Conceptual Modelling of Geothermal Systems"*, *UNU-GTP and LaGeo, Santa Tecla, El Salvador*, UNU-GTP, SC-17, 16 pp.

Teklemariam, M., 1996: *Water-rock interaction processes in the Aluto-Langano geothermal field, Ethiopia.* University of Pisa, Department of Earth Sciences, PhD thesis, 295 pp.

Teklemariam, M., Battaglia, S., Gianelli, G., and Ruggieri, G., 1996: Hydrothermal alteration in the Aluto-Langano geothermal field, Ethiopia. *Geothermics, 25-6,* 679-702.

Teklemariam, M., and Beyene, K., 2000: *Geochemical monitoring of the Aluto-Langano geothermal field, Ethiopia.* Geological Survey of Ethiopia, Addis Ababa, report., 141 pp.

UNDP, 1986: *Development of geothermal resources Ethiopia.* UNDP, report, 283 pp.

WJEC, 2015: *LA-9D well drilling report*. West Japan Engineering Consultants, Inc, Tokyo Japan, report, 39 pp.

Worku Sisay, S., 2016: *Sub-surface geology, hydrothermal alteration and 3D modelling of wells LA-9D and LA-10D in the Aluto-Langano geothermal field, Ethiopia*. University of Iceland, Reykjavík, MSc thesis, UNU-GTP, report 7, 83 pp.